

1 **Title: Rapid Evolution of Plastic-degrading Enzymes Prevalent in the Global Ocean**

2
3 **Authors:** Intikhab Alam^{1*}, Nojood Aalismail², Cecilia Martin², Allan Kamau¹, Francisco J.
4 Guzmán-Vega⁵, Tahira Jamil¹, Afaque A. Momin⁵, Silvia G. Acinas³, Josep M. Gasol³, Stefan T.
5 Arold^{5,6}, Takashi Gojobori¹, Susana Agusti⁴ and Carlos M. Duarte^{1,2*}.

6 **Affiliations:**

7 ¹Computational Bioscience Research Center (CBRC), King Abdullah University of Science and
8 Technology, Thuwal 23955, Saudi Arabia

9 ²Red Sea Research Centre (RSRC) and Computational Bioscience Research Center (CBRC),
10 King Abdullah University of Science and Technology, Thuwal 23955, Saudi Arabia

11 ³Departament de Biologia Marina i Oceanografia, Institut de Ciències del Mar-CSIC, Pg.
12 Marítim de la Barceloneta 37-49, 08003, Barcelona, Spain

13 ⁴Red Sea Research Centre (RSRC) and Computational Bioscience Research Center (CBRC),
14 King Abdullah University of Science and Technology, Thuwal 23955, Saudi Arabia

15 ⁵King Abdullah University of Science and Technology (KAUST), Computational Bioscience
16 Research Center (CBRC), Biological and Environmental Science and Engineering, Thuwal,
17 23955-6900, Saudi Arabia

18 ⁶Centre de Biochimie Structurale, CNRS, INSERM, Université de Montpellier, 34090
19 Montpellier, France

20 .
21 *Correspondence to: intikhab.alam@kaust.edu.sa, carlos.duarte@kaust.edu.sa

22
23 **Short title: Plastic-degrading Enzymes Prevalent in the Global Ocean**

24
25

26 **Abstract:**

27

28 Estimates of marine plastic stocks, a major threat to marine life (1), are far lower than expected
29 from exponentially-increasing litter inputs, suggesting important loss factors (2, 3). These may
30 involve microbial degradation, as the plastic-degrading polyethylene terephthalate enzyme
31 (PETase) has been reported in marine microbial communities (4). An assessment of 416
32 metagenomes of planktonic communities across the global ocean identifies 68 oceanic PETase
33 variants (oPETase) that evolved from ancestral enzymes degrading polycyclic aromatic
34 hydrocarbons. Twenty oPETases show predicted efficiencies comparable to those of laboratory-
35 optimized PETases, suggesting strong selective pressures directing the evolution of these
36 enzymes. We found oPETases in 90.1% of samples across all oceans and depths, particularly
37 abundant at 1,000 m depth, with a strong dominance of *Pseudomonadales* containing putative
38 highly-efficient oPETase variants in the dark ocean. Enzymatic degradation may be removing
39 plastic from the marine environment while providing a carbon source for bathypelagic microbial
40 communities.

41

42 Exponential growth in plastic production along with poor waste management practices have led
43 to over 150 Tg plastic waste delivered to the ocean since 1950 (1), where it harms marine life,
44 from zooplankton to whales (5). Synthetic plastic polymers are derived from oil hydrocarbons
45 and designed to be durable in the environment (6, 7), being largely resistant to microbial
46 degradation. However, a newly-evolved plastic-degrading enzyme, polyethylene terephthalate
47 hydrolase (PETase), was recently discovered in a Japanese waste processing plant (8). This
48 PETase was inferred to have evolved since 1970, when the polyethylene terephthalate polymer
49 was introduced at industrial scale (9). The PETase catalyzes the hydrolysis of polyethylene
50 terephthalate (PET) plastic to monomeric mono-2-hydroxyethyl terephthalate (MHET), which is
51 ultimately broken down into non-hazardous monomers, terephthalate and ethylene glycol, by
52 MHETases. The efficiency of currently known PETases seems, however, to be low, and it has
53 been suggested that in the environment it only achieves a breakdown from micro- to
54 nanoplastics, rather than full degradation (10).

55

56 The discovery, and subsequent biotechnological improvement (11) of this spontaneously-evolved
57 plastic-degrading enzyme offers hope that plastic waste can be degraded in waste facilities,
58 thereby preventing it from entering the ocean (12). However, this still leaves the fate of the > 150
59 Tg plastic waste already delivered to the ocean unresolved. Recent estimates show that 99% of
60 the plastic that entered the oceans cannot be accounted for, since inventories of plastic floating
61 on the surface of the ocean account to ~ 1% of the expected load (2), pointing at the operation of
62 processes responsible for major losses of plastic at sea (3). One such process may involve the
63 microbial degradation of plastics. Microplastics, the numerically dominant marine debris, have
64 developed a characteristic microbial community, referred to as the marine plastisphere (10). If
65 the PETase enzyme evolved in waste treatment plants from ancestral *Ideonella sakaiensis* (*I.*
66 *sakaiensis*) genes (8), and provided the current prevalence of polyethylene terephthalate as debris
67 in the marine environment, it is possible that other PETases may have evolved independently in
68 plastisphere ocean microbes as well. The huge population of prokaryotes in the global ocean,
69 estimated to contribute 10^{29} cells distributed among 10^{10} different OTUs (13), provides enough

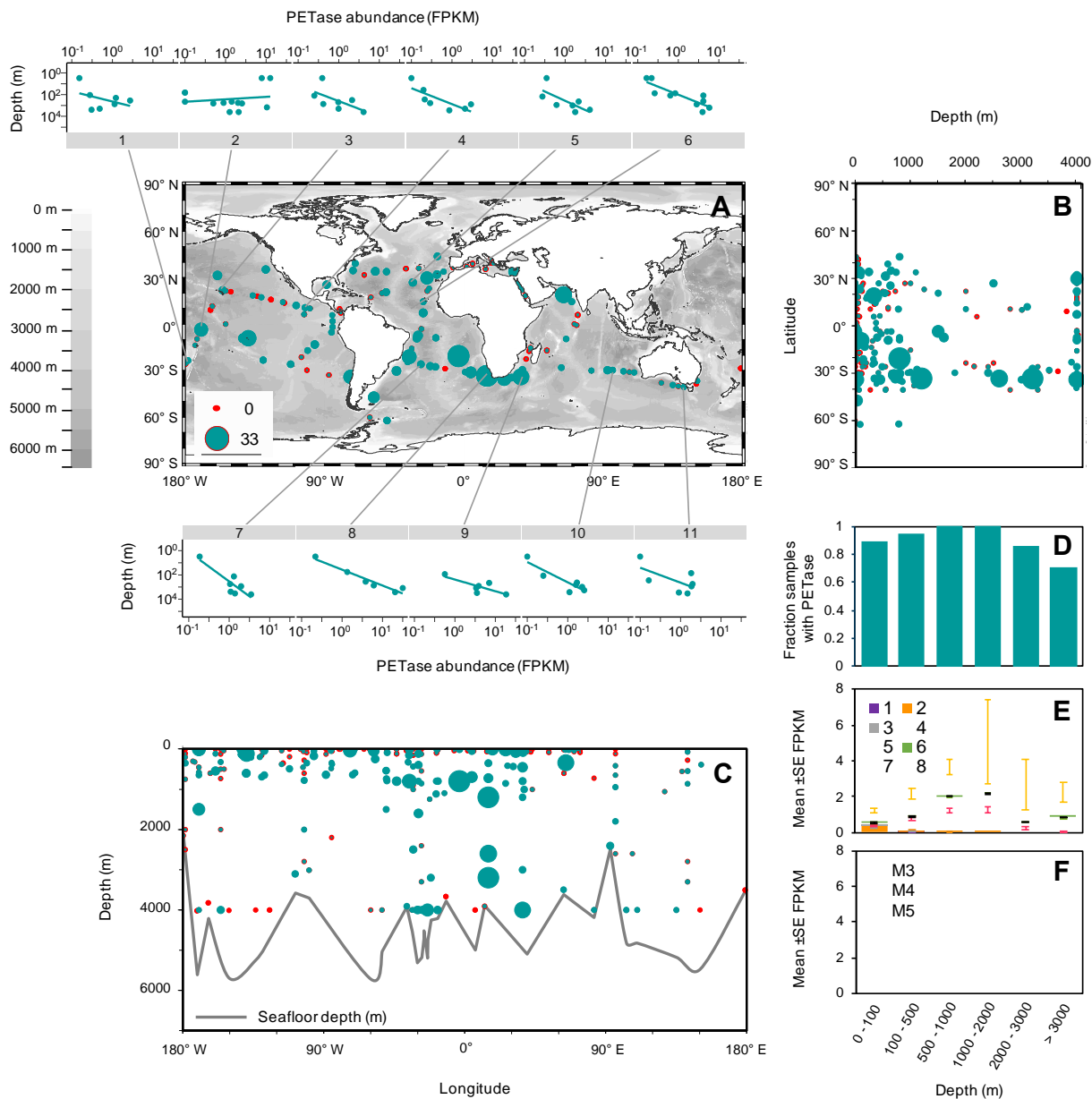
70 population size, genetic diversity and rate of growth for mutations(14) to independently evolve
71 PETase activity, which would enable microorganisms to access a novel, widely available organic
72 substrate. Indeed, a recent assessment of PETase abundance in marine and terrestrial
73 environments, confirmed the presence of the PETase gene in 31 of the 108 environmental marine
74 samples examined, all from surface waters (4). However, a global assessment of the presence,
75 abundance and diversity of PETases in the whole ocean, extending to the deep ocean, the largest
76 microbial habitat in the biosphere (15), is yet to be conducted.

77

78 **Results**

79 Here we report the prevalence of PETases in the global ocean microbiome and provide a
80 phylogeny suggesting Oceanospirillales to be the parental clade leading to 68 identified variants
81 of marine PETase. We do so on the basis of a thorough exploration of PETase through gene
82 catalogs from two global-ocean expeditions, *Tara Oceans* (16) and *Malaspina* (17), delivering
83 416 metagenomes collected from 204 individual ocean locations across the Indian, Pacific and
84 Atlantic Oceans from surface to the deep sea (Fig. 1).

85



86

87

88 **Fig. 1** (A) Global distribution of PETase (in FPKM) in marine metagenomes. The scale also applies to panels B
 89 and C. The 11 small plots show the distribution of PETase genes across depth (m) in 11 profiles collected during the
 90 Malaspina Expedition. (B) Distribution of PETase along depth and latitude and (C) along depth and longitude. The
 91 grey line in panel C shows the seafloor depth (m) as it compares to the deepest sampling point. (D) Fraction of
 92 samples with PETase and mean \pm SE PETase abundance (in FPKM) per (E) taxonomic group and (F) Abundance of
 93 oPETases assigned with Motif groups M3-5 (set of motifs designed to capture PETase characteristic catalytic triad
 94 and other features) at 6 depth layers (0 - 100 m, 100 - 500 m, 500 - 1000 m, 1000 - 2000 m, 2000 - 3000 m and
 95 > 3000 m). Taxonomic groups, identified as numbers from 1 to 8 in panel E, correspond to the following bacterial
 96 orders: 1. Candidatus Poribacteria_UO; 2. Flavobacteriales; 3. Gammaproteobacteria_UO; 4.
 97 Gemmatimonadetes_UO; 5. Oceanospirillales; 6. Phycisphaerales; 7. Planctomycetales; 8. Pseudomonadales.

98

99 Using the KAUST Metagenomic Analysis Platform (KMAP) we queried our pre-annotated *Tara*
100 Oceans and Malaspina gene catalogs for the presence of *Ideonella sakaiensis* PETase (EC
101 3.1.1.101)-like enzymes containing the Dienelactone hydrolase (DLH) domain. DLH is a generic
102 α/β -hydrolase domain present in many hydrolases, but in the case of PETase it contains a
103 signature catalytic triad (https://pfam.xfam.org/protein/PETH_IDESA, Fig 2a) (4). The DLH
104 domain is present in more than 17,000 sequences in the Pfam database
105 (<https://pfam.xfam.org/family/PF01738>, accessed Feb 2, 2020). However, most of these
106 sequences are related to genes coding for enzymes involved in the degradation of hydrocarbons.
107 Only one DLH form, harboring specific substitutions in the catalytic triad (motif residues S, D
108 and H) has been experimentally confirmed to degrade PET (4), Fig 2a).

109

110 **Diversity and efficiency of oceanic PETase**

111

112 Our analysis yielded 75 candidate PETases in the *Tara* Oceans and Malaspina gene catalogues.
113 These gene catalogs were annotated based on full sequence comparisons to public databases.
114 Based on manual inspection of alignments from these 75 oceanic candidate oPETases and 8
115 known homologs (4) of *I. sakaiensis* PETase we defined five overlapping generic to specific
116 PHI-BLAST searchable motifs, M1-5 (Fig 2a, 2d). Motifs M1 and M2 detect PETase-like
117 sequences but miss the catalytic triad, the main component of known PETases (4). Motif M3
118 include the catalytic triad, conserved central motif GGGG as well as the oxyanion hole residues
119 and the aromatic clamp. Two exceptions are oPETase 72 and 75 where catalytic triad appears to
120 be available but the conserved motif GGGG is modified to GG-[AG]-[GA]. M4 is similar to M3
121 but contains the [PG]-G-[YF] motif that defines an additional aromatic clamp and oxyanion hole
122 upstream of the catalytic triad. M5 is the largest motif. It includes M3 and M4 and additionally
123 contains a conserved DxRxR(Y)xxF(L)C sequence, preceding a region providing thermostability
124 to the enzyme (Fig 2a, 2d). Because of the requirement for the catalytic triad of PETases degrade
125 PET, putative PETases containing only motifs M1 and M2 were discarded. Only those with
126 motifs including the catalytic triad (M3, M4 or M5) were considered as functional PETases. This
127 selection yielded 68 variants of putative functional PETases present in the *Tara* Ocean and
128 Malaspina gene catalogues (Suppl. Table 1). Alignments of these oPETases from motif groups
129 M3-5 and shown in Figure 2-supplement 1.

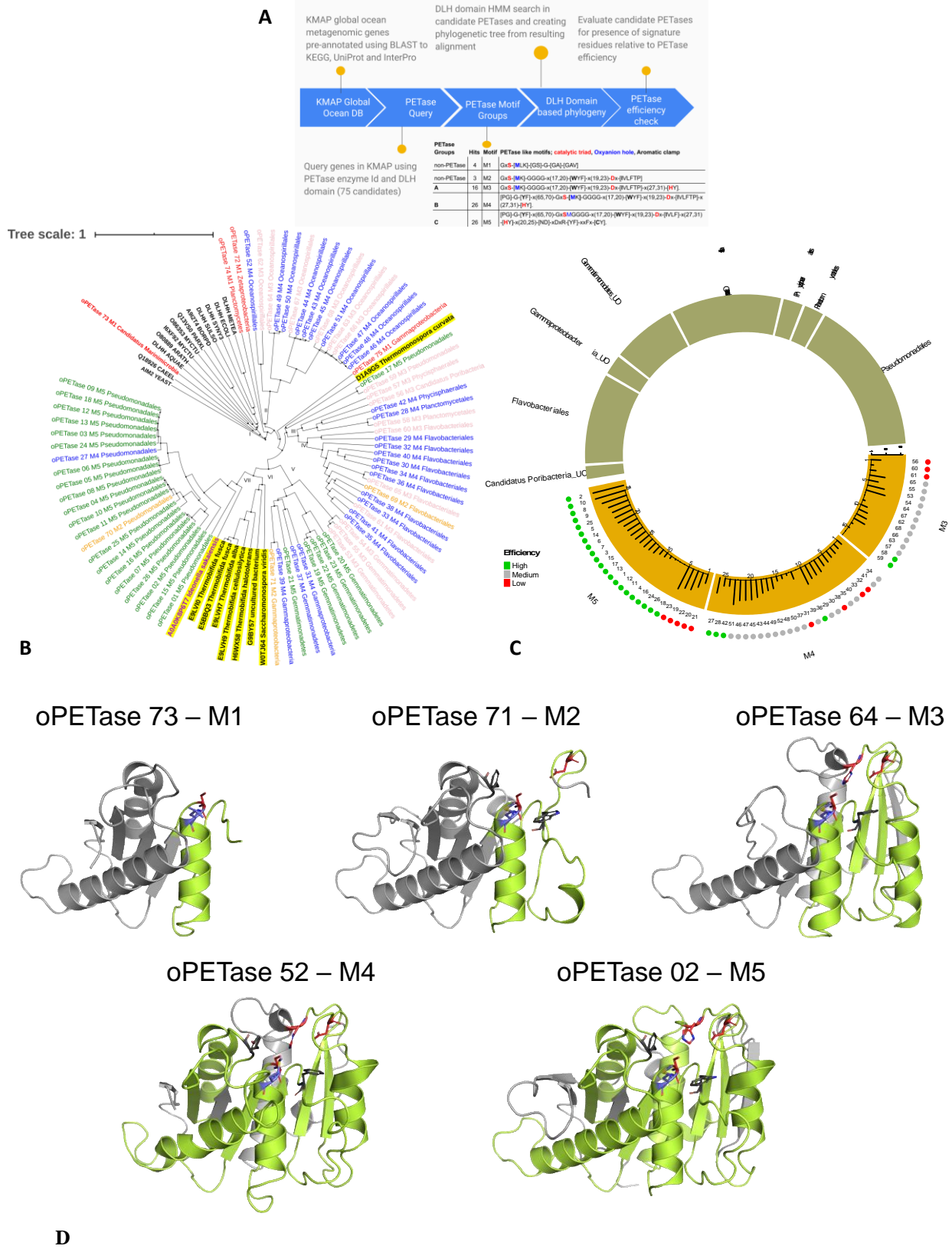
130

131 Scoring of candidate oPETases (see Methods and Suppl. Table S2-3) consistently designated
132 most of the oPETases containing Motif 5 as having a predicted efficiency score close to or
133 slightly above that of the reference *I. sakaiensis* PETase (4), which also contains M5 (Suppl.
134 Table S2). Most of the key residues that are essential for PETase activity are largely conserved
135 across the 68 functional variants. Most of the oPETase variants predicted to be efficient
136 contained M5 (Fig. 2c). Moreover, we found that 20 of the newly identified oPETases, many of
137 which had the M5 motif, already displayed residue substitutions that were identified as
138 enhancing PETase activity in engineered laboratory variants of *I. sakaiensis* PETases (18)
139 (Suppl. Table S3).

140

141 To support and inform the scoring process, high-confidence structural homology models were
142 also produced for all putative PETases, using SWISS-MODEL (19), based on up to 50%
143 sequence identity with the crystal structure of the IsPETase in a complex with HEMT (PDB ID
144 5xh3 (20)). The structural analysis of potential oPETases can be described using one of the high
145 scoring oPETase example such as oPETase_02. This selected putative PETase contains the
146 catalytic triad (S160, D206, H237) and the disulfide bond linking residues C203 and C239,
147 demonstrated to be essential for PETase function (20, 21)(Fig. 2d). In addition, it harbors two
148 modifications that were shown to increase the catalytic activity of IsPETase (22), namely R90A
149 and L117F. The R90A modification is thought to reduce the steric hindrance around the active
150 site and increase the hydrophobic area to facilitate the accumulation of substrate near the
151 substrate-binding cleft. The L117F modification stabilizes Y87 (F87 in this case), which
152 enhances the interaction between the enzyme and the substrate, as shown by a lower Michaelis
153 constant, K_m of the L117F mutant as compared to the wild-type PETase. The S214H variant
154 found in some oPETases has been seen to reduce PETase activity, possibly because the larger
155 His restricts the movement of the adjacent W185 (20). Also, other variants that have not been
156 experimentally tested were found in these oPETases (see Supp. Table S1), and their effect on the
157 catalytic activity of the protein remains uncertain. The variants Y87F, T88V and S238Y/F
158 increase the hydrophobicity around the active site, which is expected to be beneficial for PETase
159 activity, as were other substitutions increasing the hydrophobicity of this region, as they may
160 facilitate the interaction of the enzyme with the substrate. The R280Q substitution in most of the
161 higher-scoring variants is conservative and not expected to influence catalysis, and other
162 important positions such as W159, W185 and M161 remain unchanged in these variants. Overall,
163 the compound effects of these modifications make these variants good PETase candidates with a
164 chance of having a PET degrading activity close to or potentially better than IsPETase. It is
165 however important to note that our predicted efficiency scores of these oPETases to rank
166 potentially better or worse cases are adapted based on the presence of favorable or inhibiting
167 mutations only, and that an experimental validation is needed to confirm real efficiency of these
168 oPETases.

169



170

171

172 **Fig. 2.** Overview, Phylogenetics and efficiency analysis of candidate Ocean PETases (oPETases). (A) An overview
173 of our workflow in exploring oPETases. (B) Phylogenetic analysis of DLH-containing PETases. Here sequence
174 names are colored according to associated Motifs M1-5 (M1 in red, M2 in orange, M3 in pink, M4 in blue and M5
175 in green). DLH seed sequences are in black, similarly known PETases are in black but highlighted in yellow, the
176 original *I. sakaiensis* PETase sequence is in purple and highlighted in yellow. Roman numbers indicate the 7 clades
177 in which PETases are grouped (C) Analysis of candidate oPETases is shown for motif groups M3, M4 and M5
178 (lower half of the circle) presenting potential for efficiency (outer lower circle) as green, grey and red dots depicting
179 high, medium and low efficiency categories, respectively. For potential efficiency to degrade PET, based on the
180 evaluation of only critical residues, see Suppl. Table S2 and efficiency scoring scheme. Total gene abundance for
181 each of these oPETases in ocean is shown in respective bar graphs with orange background. Associated taxonomic
182 information (upper half of the circle) is linked to oPETase motif groups through colored ribbons (M3 is green, M4 is
183 blue and M5 is shown in pink). (D) An illustration of protein structures representative of each motif category, with
184 the corresponding motif M1 to M5 colored in lime green. The models were obtained by SWISS-MODEL based on
185 the crystal structure of IsPETase in complex with HEMT (PDB ID 5xh3) as a template. Key residues are shown as
186 stick models, color-coded as follows: red, the catalytic triad; blue, the Met residue involved in the oxyanion hole;
187 dark grey: residues forming the aromatic clamp, where [YF]87 is part of both the aromatic clamp and the oxyanion
188 hole.

189

190 **Phylogeny and evolution of efficient oceanic PETase**

191 We established a phylogenetic tree of all PETase sequences, including all Motifs 1 to 5, to
192 investigate the evolutionary pathway from the ancestral DLH domain to fully functional PETase
193 domains including the signature catalytic triad. The phylogenetic tree included the 75 candidate
194 PETases identified in the *Tara* Oceans and Malaspina gene catalogues, the original *I. sakaiensis*
195 PETase sequence (8), the eight land-derived homologues reported from the uniprot database (4),
196 and 12 non-PETase DLH domain core sequences from the Pfam database as an outgroup (Fig.
197 2b). The resulting phylogenetic tree identified the 12 non-PETase DLH domain core sequences
198 together with two out of three of those containing Motif 1 as a parental group from which
199 PETases evolved, hereafter defined as clade I (Fig. 2b). All other clusters defining six additional
200 taxonomic PETase clades of fully-functional PETases containing M3 to M5 (Fig. 2b), as well as
201 three sequences containing non-functional PETase M2 motifs, interspaced among M3 to M5-
202 containing sequences (Fig. 2b). Clade II is dominated by Oceanospiriales, Clade III contains a
203 mixture of taxa, Clade IV contains Flavobacteriales, Clade V contains Gemmatimonadetes and
204 Gammaproteobacteria, Clade VI contains the eight previously defined homologues of *I*
205 *sakaiensis* PETase from land microbes (4), with an additional such homologue
206 (*thermomonospora curvata*, D1A9G5) clustering with clade III (Fig. 2b). Cluster VII contains
207 the original *I. sakaiensis* PETase sequence along with Pseudomonadales sequences, all except
208 two, containing the Motif 5 (Fig. 1b).

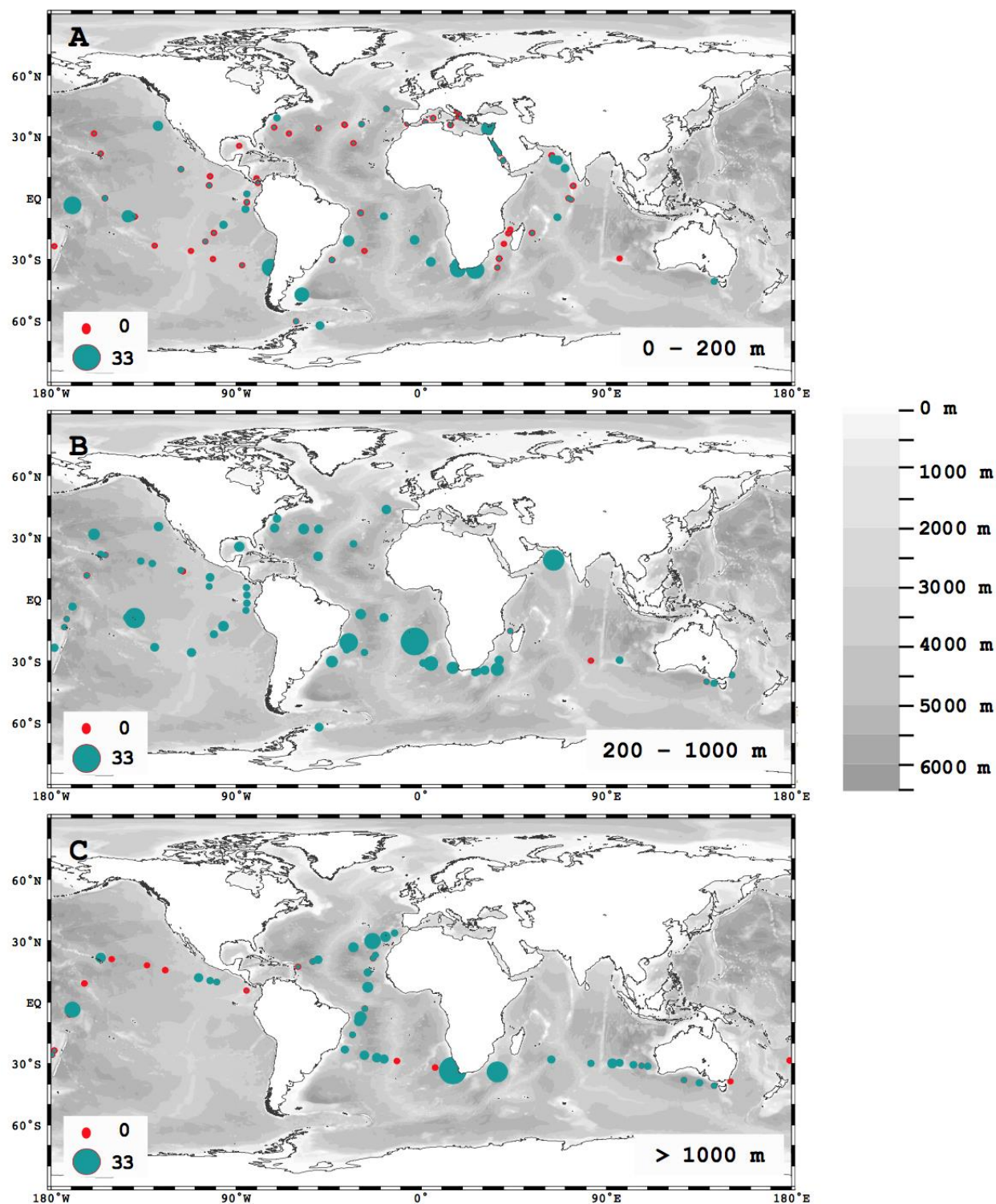
209

210 In summary, the order of clusters in the phylogenetic tree represents a putative evolutionary
211 progression from DLH-containing ancestors to the eight bacterial orders containing putatively
212 functional oPETases (Fig. 2b). Specifically, the phylogenetic tree obtained suggests that PETases
213 evolved from M1 and M2 DLH-containing sequences of genes involved in the degradation of
214 naturally-occurring hydrocarbons present in the ocean prior to synthetic PET addition to the
215 ocean. The PETases appear to have evolved in parallel in six major independent clades (clades II
216 to VII), all of which include functional PETase motifs (M3, M4 and M5). The phylogenetic tree
217 shows an enrichment of the clades in Motif 5 from clade V, where it first appears, to the clade
218 VII, where all (except one *Pseudomonadales* sequence) include M5. Our analysis points at

219 *Pseudomonadales* containing efficient variants of PETase, as the fundamental outcome of the
220 processes driving the evolution of efficient PETase in the ocean, here oPETase variants 2 and 10
221 were found to be most abundant (Fig 2c).

222
223 **Distribution and abundance of PETases in the global ocean**

224 PETases were prevalent in marine metagenomes, present in 90.1% of the samples assessed,
225 across all oceans and depths sampled (Fig. 1). PETases were present from the surface to the deep
226 sea (Fig. 1b, c), with both prevalence and abundance reaching a maximum at the base of the
227 permanent thermocline (1,000 m depth, Fig. 1d, e), thereby showing a tendency to increase
228 toward the ocean interior (mixed-effect model, slope for depth = 2.979, P = 0.0133, 11 plots in
229 Fig. 1a). This analysis is based on 11 sampling points, where samples were collected at different
230 depths leading to 11 profiles, 10 of which show that PETase abundance increases with depths.
231 PETase abundance in the upper ocean (< 200 m) was highest around South America, South
232 Africa, India, French Polynesia and the Red Sea (Fig. S2a), and PETase abundance in the deep-
233 sea was greatest in the Atlantic Ocean, followed by the Indian Ocean (Fig. S2). Some of these
234 areas, including Southern Africa (23) and Indian subcontinent (24), have been reported to be
235 areas of high abundance of microplastics.



236

237 **Fig. 3.** Global distribution of PETase (in FPKM) in marine metagenomes of (A) surface (0 - 100 m), (B)
238 mesopelagic (200 - 1,000) and (C) deep waters (> 1000m).

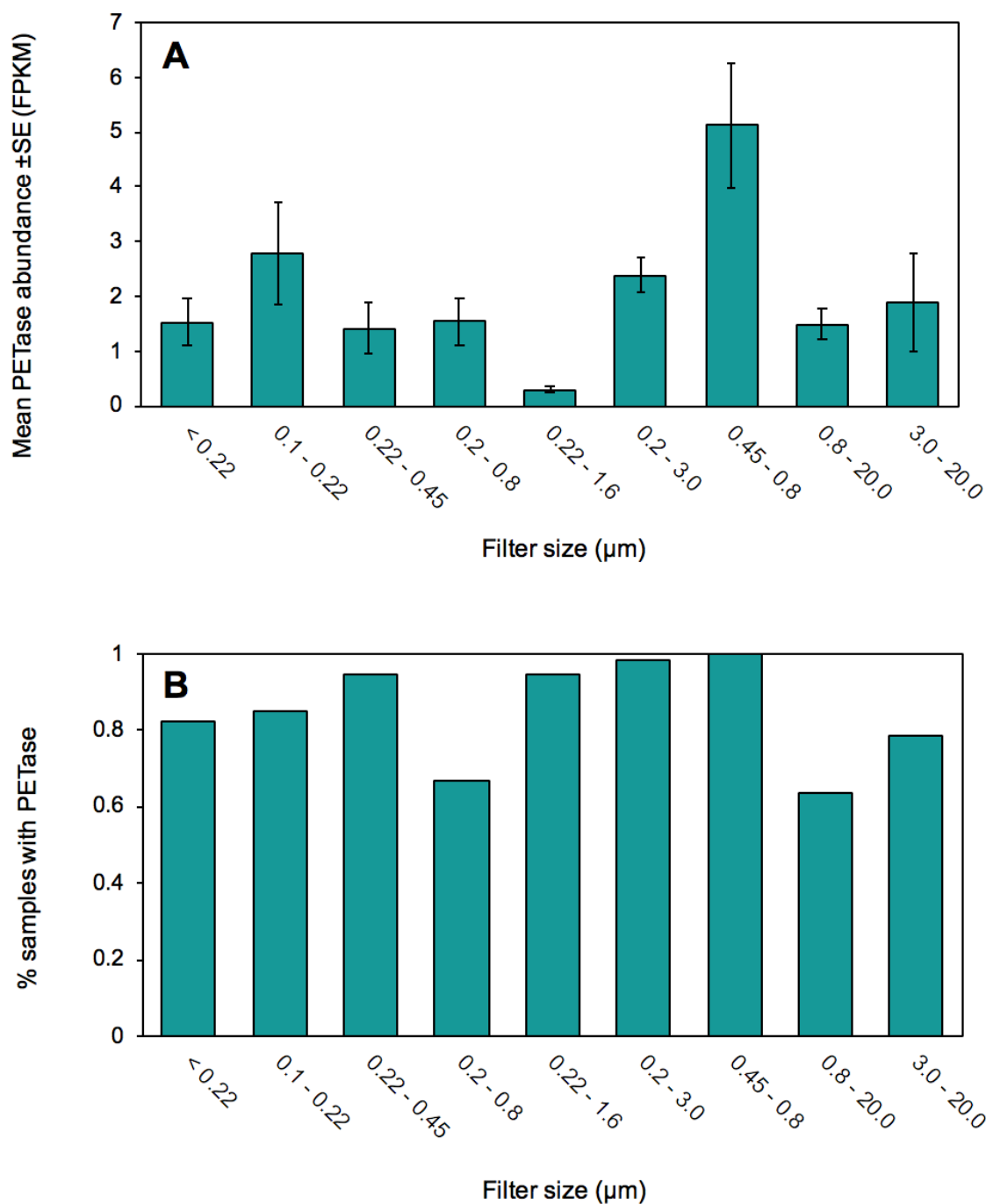
239 The distribution of PETase contained within *Proteobacteria* was relatively uniform across depth
240 layers (Fig. 1e), however the distribution of PETase contained within *Gemmatimonadetes*
241 increases with depth up to 2,000 m and declines slightly in deeper waters. PETases contained

242 within *Bacteroidetes* were restricted to water depths shallower than 1,000 m (Fig. 1e). PETase-
243 containing *Proteobacteria*, the prokaryote class with the highest abundance and prevalence of
244 PETases, was, in turn, dominated by *Pseudomonadales*, containing efficient M5 motifs, and
245 *Oceanospirillales* orders, with an unidentified order within *Gemmatimonadetes* also contributing
246 considerably to PETase abundance in the mesopelagic ocean (Fig. 1e, Table S1). There was no
247 clear difference in PETase abundance and prevalence between particle attached ($> 3 \mu\text{m}$) and
248 free-living communities ($< 3 \mu\text{m}$, Wilcoxon Rank Sum Test, $W = 2892.5$, $p\text{-value} = 0.46$).
249 PETase variants containing the efficient M5 module were dominant across all depth layers (Fig.
250 1f), with PETase variants containing the M3 variant being the least abundant in oceanic
251 microbial communities (Fig. 1f).

252

253 The taxonomy of oPETases differs from that of PETase containing bacteria in other
254 environments. A previous search of 8 homologues of *I. sakaiensis* PETases, all containing the
255 M5 motif, in the public NCBI non-redundant protein database retrieved ~500 PETase-like
256 sequences (4), largely corresponding to microbial communities sampled from terrestrial habitats
257 and related to *Actinobacteria*. An updated search in NCBI (accession date, December 2019),
258 resulted in twice the number of sequences (1138 sequences), also mostly corresponding to soil
259 *Actinobacteria* (1040 sequences). However, ~86 hits appear to be related with proteobacteria
260 (Suppl. Table 4). Our analysis of the phylogeny and abundance of oPETases compared with the
261 results from NCBI clearly show that the PETase-containing ocean microbial community differs,
262 and that PETases likely evolved independently on land and in the ocean.

263



264

265 Fig. 4. (A) Mean PETase abundance \pm SE (FPKM) and (B) prevalence of samples where PETase occurred in each of
266 9 filter sizes (μ m).

267 Our sampling of metagenomes does not allow to directly link the PETase containing microbes to
268 plastic particles. However, our samples are likely to all contain plastic particles. Indeed, as the
269 global metagenomes assessed were retrieved by filtering large volumes of seawater onto filters
270 of different sizes (Fig. 4), any plastic particle, whether marine micro- (< 5 mm) or nanoplastics
271 (< 0.1 μ m) (25), present in the water would also be retained. Especially, filters would have
272 retained synthetic fibers (about 0.2 to several mm long and less than 50 μ m in diameter), which

273 are the most abundant debris in the ocean, present in the water at concentrations of about 100 to
274 300 fibers per liter (26). A review of the microbial communities found in the oceanic plastisphere
275 shows that *Pseudomonadales* and *Flavobacteriales*, which our analysis showed that may contain
276 the efficient M5 and M4/M3 PETase, respectively (Fig. 2c), have been detected to form biofilms
277 on marine microplastics sampled in the North Atlantic (27) and North Sea (28). In addition,
278 *Gammaproteobacteria*, which our analysis showed contain the M4-containing PETases (Fig. 2c),
279 have been also reported growing in microbial films on marine microplastics from the Baltic Sea
280 (29), the Caribbean Sea (30), at the coastline of Singapore (31), and through the great Pacific
281 garbage patch (32). However, *Oceanospirillales*, which our analysis showed contain M3 and M4
282 variants of the PETase, have been identified only in marine plastic-associated bacterial
283 communities in the North Atlantic (27).

284

285 In summary, the results obtained confirm that PETases are prevalent and abundant in the global
286 ocean microbiome, where they must have evolved recently, following the mass production of
287 polyethylene terephthalate (9). PETases are widespread from the surface to the deep ocean,
288 reaching a maximum abundance and prevalence at about 1,000 m, where *Pseudomonas* has
289 evolved an efficient PETase. PETases were found in high abundance in some areas known to
290 receive high loads of plastic waste, such as waters off the Indian subcontinent, Brazil, and
291 Southern Africa. The phylogeny constructed also shows a putative pathway for the evolution of
292 oPETases from ancestral genes involved in hydrocarbon degradation. The increased efficiency of
293 the PETase along the phylogenetic sequences, along with the high abundance of bacteria
294 containing efficient PETases, points at an ongoing evolutionary process driven by selection
295 pressures providing advantages to bacteria able to use an increasingly available resource, plastic
296 polymers, in the deep ocean, mainly where all other naturally-occurring organic substrates are
297 extremely diluted (33). The widespread prevalence, 90.1%, of PETases across the ocean
298 together with the acute carbon limitation in bathypelagic waters suggests that the ocean
299 microbiome is rapidly evolving to degrade plastic waste, providing a hopeful, nature-based
300 solutions for plastic already in the marine environment.

301

302 **Materials and Methods**

303 **Data collection and DMAP based annotation**

304 Metagenome data was retrieved from two global expeditions, the TARA Oceans expedition,
305 which sampled the upper layer of the ocean from sail-boat *Tara* (16) and the Malaspina
306 Expedition, which sampled open ocean waters extending down to 4,000 m depth from Spanish
307 R/V *Hesperides* (17). The metagenomic data-sets included 243 metagenome samples from
308 TARA and 173 metagenomes from the MALASPINA expedition, ranging from surface down to
309 4,000 m depth and including samples from all oceans (Fig. 1). These samples were used to
310 investigate the prevalence of PETase genes. Samples were filtered through different filter sizes
311 (<0.22, 0.1 - 0.22, 0.22 - 0.45, 0.2 - 0.8, 0.22 - 1.6, 0.2 - 3, 0.45 - 0.8, 0.8 - 3.0, 3.0 - 20.0 μm)
312 to explore the abundance and prevalence of PETase genes in each fraction and especially in
313 particle attached (> 3 μm) and free-living communities (< 3 μm). Non-redundant Gene catalogs
314 from MP and MD samples were obtained by assembly using MegaHit (34) and gene prediction
315 for each of the samples, followed by pooling of sample specific genes through CD-HIT based
316 clustering (95% nucleotide identity and 80% overlap of the shorter sequence). TARA oceans

317 microbial gene catalog was already available with 40 million genes. MP and MD gene catalogs
318 produced a non-redundant set of 32 and 11 million genes, respectively. These gene catalogs were
319 annotated using DMAP where taxonomic affiliation of every gene is investigated using Least
320 Common Ancestor estimation through BLAST against UniProtKB database. Functional
321 annotation is obtained through BLAST matches to KEGG sequences with defined KEGG
322 Orthologs (KO) and identification of domains using InterPro (35). These Taxonomic and
323 Functional annotations including cross references, such as Enzyme Classification (E.C), Gene
324 Ontology (GO) and BLAST statistics (Evalue, Percent Identity and Percent Coverage) are saved
325 in to Gene Information Table (36) format, ready to be indexed for browsing and comparison
326 through DMAP compare module. To estimate gene abundance counts as Fragments per Kilobase
327 normalized to one Million (FPKM), reads were mapped on to their respective gene catalogs from
328 individual samples in strictly paired mode using bbmap.

329

330 **Analysis of plastic degrading-related genes**

331 **PETase abundance in global ocean metagenomes**

332 We queried TARA, MP and MD gene catalogs to obtain list of non-redundant genes considering
333 enzyme label 3.1.1.101, KEGG Ortholog (KO) K21104 restricted to hits with Pfam signature
334 domain ‘Dienelactone hydrolase family’ with PFAM ID PF01738. Table S1 shows the count of
335 non-redundant genes found as a result of this search. This same query was used in DMAP to
336 obtain gene abundance estimates from individual samples.

337

338 **Phylogeny analysis**

339

340 A protein sequence set of all non-redundant PETase related 75 genes, obtained through querying
341 DMAP, was combined with *I. sakaiensis* PETase gene, its 8 homologs (from (4)) and as an
342 outgroup 12 seed sequences from DLH domain were included. An alignment of sequences was
343 performed using hmmsearch with DLH domain as a query. Resulting alignment was converted
344 into fasta format and a phylogenetic tree was built using mafft phylogeny option at
345 <https://mafft.cbrc.jp/alignment/server/phylogeny.html> . The alignment was colored based on
346 different motif groups, *Ideonella sakaiensis* PETase with homologs and seed sequences from
347 DLH domain.

348

349 **Efficiency scoring and homology modelling**

350

351 A scoring system was developed to rank the candidate oPETases, 8 known PET hydrolases, and
352 12 seed sequences containing the DLH domain. This scoring was made by comparison to the
353 PETase sequence from *I. sakaiensis* (IsPETase), taking into account some of the key residues
354 that are known to contribute to the activity and stability of IsPETase, as well as variants and
355 mutations that have been experimentally tested and yielded either an increase or decrease in its
356 ability to degrade PET (Supplementary Methods and Suppl. Table S2-3). The scoring was then
357 performed with the following considerations: Given the difficulties to predict how the presence

358 of additional varying residues in the sequence with respect to IsPETase might affect the
359 performance of the experimentally tested mutations as reported in the literature, the scoring was
360 applied as a count or sum of the number of positive mutations (i.e. enhancing PETase activity)
361 minus the number of negative mutations (i.e. inhibiting PETase activity). Additionally, a higher
362 weight was given to the residues composing the catalytic triad and the PETase-specific disulfide
363 bond, and a higher penalty to their absence. A labelling of PETases based on resulting score
364 binned into low, medium and high efficiency, depicted by red, grey and green colors,
365 respectively, is shown in Fig. 1c. After several rounds of scoring varying different parameters,
366 such as the number of mutations/key amino acids considered and the weights given to each
367 residue, the ranking of the analyzed sequences was proven to be robust.

368

369 **Acknowledgments:** We are thankful to KAUST Supercomputing Laboratory (KSL) for
370 providing computational resources need to carry out this work, **Funding:** The research reported
371 in this publication was supported by funding from King Abdullah University of Science and
372 Technology (KAUST), Office of Sponsored Research (OSR), under award number URF/1/1976-
373 21-01, and the Malaspina Circumnavigation Expedition funded by the Spanish Ministry of
374 Economy and Competitiveness (CSD2008-00077); **Author contributions:** IA and CMD
375 conceived the study, SGA. JMG, TG, CMD and SA contributed data, IA, AK, CMD, NA, CM
376 and TJ analyzed the metagenome data, FJGV, AAM and STA conducted the structural modelling
377 and efficiency assessment, IA, CMD, NA and CM wrote the first draft of the paper and all
378 coauthors contributed to improve the paper and approved the submission; **Competing interests:**
379 Authors declare no competing interests; and **Data and materials availability:** All data are
380 available (see sequence data information in M&M).

381

383 References

- 384
- 385 1. F. Gallo *et al.*, Marine litter plastics and microplastics and their toxic chemicals
386 components: the need for urgent preventive measures. *Environ Sci Eur* **30**, 13 (2018).
- 387 2. E. van Sebille *et al.*, A global inventory of small floating plastic debris. *Environmental*
388 *Research Letters* **10** (2015).
- 389 3. M. W. Ryberg, M. Z. Hauschild, F. Wang, S. Averous-Monnery, A. Laurent, Global
390 environmental losses of plastics across their value chains. *Resources, Conservation and*
391 *Recycling* **151** (2019).
- 392 4. D. Danso *et al.*, New Insights into the Function and Global Distribution of Polyethylene
393 Terephthalate (PET)-Degrading Bacteria and Enzymes in Marine and Terrestrial
394 Metagenomes. *Appl Environ Microbiol* **84** (2018).
- 395 5. S. C. Gall, R. C. Thompson, The impact of debris on marine life. *Mar Pollut Bull* **92**,
396 170-179 (2015).
- 397 6. D. K. Barnes, F. Galgani, R. C. Thompson, M. Barlaz, Accumulation and fragmentation
398 of plastic debris in global environments. *Philos Trans R Soc Lond B Biol Sci* **364**, 1985-
399 1998 (2009).
- 400 7. B. Gewert, M. M. Plassmann, M. MacLeod, Pathways for degradation of plastic
401 polymers floating in the marine environment. *Environ Sci Process Impacts* **17**, 1513-
402 1521 (2015).
- 403 8. S. Yoshida *et al.*, A bacterium that degrades and assimilates poly(ethylene terephthalate).
404 *Science* **351**, 1196-1199 (2016).
- 405 9. H. P. Austin *et al.*, Characterization and engineering of a plastic-degrading aromatic
406 polyesterase. *Proc Natl Acad Sci U S A* **115**, E4350-E4357 (2018).
- 407 10. L. A. Amaral-Zettler, E. R. Zettler, T. J. Mincer, Ecology of the plastisphere. *Nat Rev*
408 *Microbiol* **18**, 139-151 (2020).
- 409 11. M. Furukawa, N. Kawakami, A. Tomizawa, K. Miyamoto, Efficient Degradation of
410 Poly(ethylene terephthalate) with *Thermobifida fusca* Cutinase Exhibiting Improved
411 Catalytic Activity Generated using Mutagenesis and Additive-based Approaches. *Sci Rep*
412 **9**, 16038 (2019).
- 413 12. M. U. Sheth *et al.*, Bioengineering a Future Free of Marine Plastic Waste. *Frontiers in*
414 *Marine Science* **6** (2019).
- 415 13. K. J. Locey, J. T. Lennon, Scaling laws predict global microbial diversity. *Proc Natl*
416 *Acad Sci U S A* **113**, 5970-5975 (2016).
- 417 14. D. L. Kirchman, Growth Rates of Microbes in the Oceans. *Ann Rev Mar Sci* **8**, 285-309
418 (2016).
- 419 15. B. N. Orcutt, J. B. Sylvan, N. J. Knab, K. J. Edwards, Microbial ecology of the dark
420 ocean above, at, and below the seafloor. *Microbiol Mol Biol Rev* **75**, 361-422 (2011).
- 421 16. E. Karsenti *et al.*, A holistic approach to marine eco-systems biology. *PLoS Biol* **9**,
422 e1001177 (2011).
- 423 17. C. M. Duarte, Seafaring in the 21st century: the Malaspina 2010 circumnavigation
424 expedition. *Limnology and Oceanography Bulletin* **24**, 11-14 (2015).
- 425 18. H. Seo *et al.*, Production of extracellular PETase from *Ideonella sakaiensis* using sec-
426 dependent signal peptides in *E. coli*. *Biochemical and Biophysical Research*
427 *Communications* **508**, 250-255 (2019).

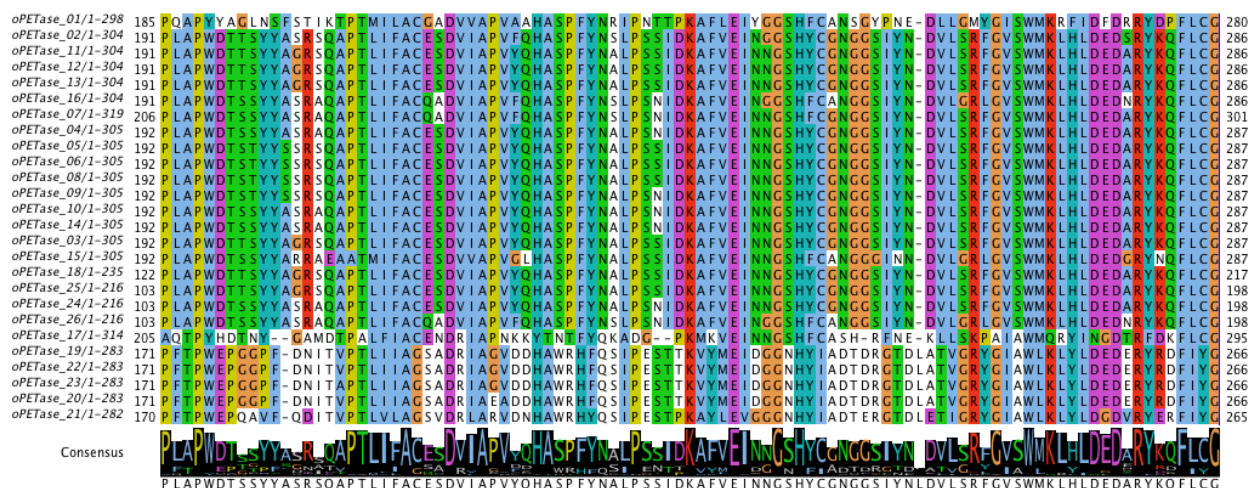
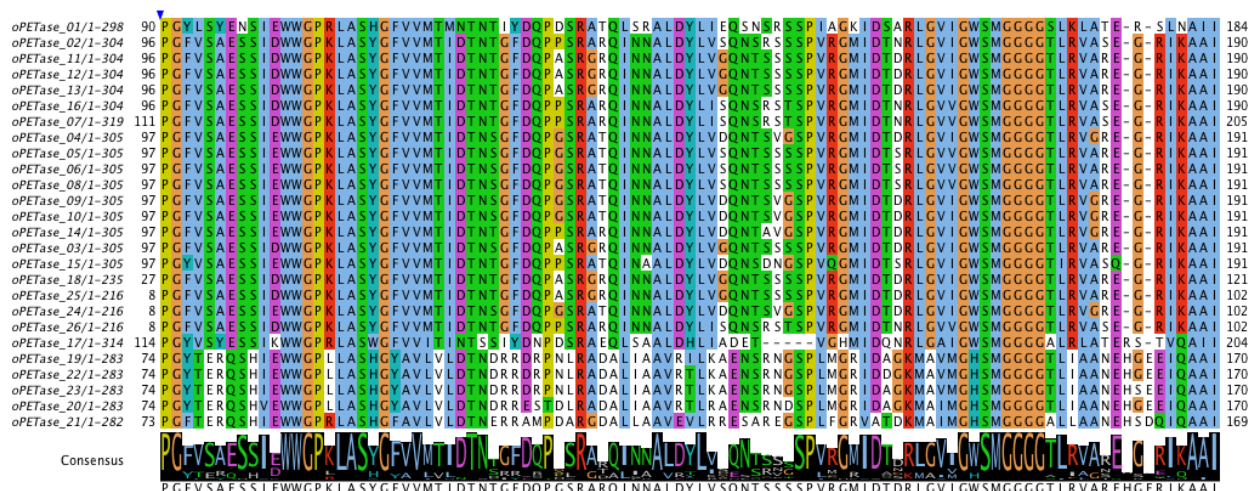
- 428 19. A. Waterhouse *et al.*, SWISS-MODEL: homology modelling of protein structures and
429 complexes. *Nucleic Acids Research* **46**, W296-W303 (2018).
- 430 20. X. Han *et al.*, Structural insight into catalytic mechanism of PET hydrolase. *Nat Commun*
431 **8**, 2106 (2017).
- 432 21. S. Joo *et al.*, Structural insight into molecular mechanism of poly(ethylene terephthalate)
433 degradation. *Nat Commun* **9**, 382 (2018).
- 434 22. Y. Ma *et al.*, Enhanced Poly(ethylene terephthalate) Hydrolase Activity by Protein
435 Engineering. *Engineering* **4**, 888-893 (2018).
- 436 23. C. Verster, K. Minnaar, H. Bouwman, Marine and freshwater microplastic research in
437 South Africa. *Integrated Environmental Assessment and Management* **13**, 533-535
438 (2017).
- 439 24. F. Shahul Hamid *et al.*, Worldwide distribution and abundance of microplastic: How dire
440 is the situation? *Waste Management & Research* **36**, 873-897 (2018).
- 441 25. A. A. de Souza Machado, W. Kloas, C. Zarfl, S. Hempel, M. C. Rillig, Microplastics as
442 an emerging threat to terrestrial ecosystems. *Global Change Biology* **24**, 1405-1416
443 (2018).
- 444 26. M. A. Browne *et al.*, Accumulation of Microplastic on Shorelines Worldwide: Sources
445 and Sinks. *Environmental Science & Technology* **45**, 9175-9179 (2011).
- 446 27. E. R. Zettler, T. J. Mincer, L. A. Amaral-Zettler, Life in the “Plastisphere”: Microbial
447 Communities on Plastic Marine Debris. *Environmental Science & Technology* **47**, 7137-
448 7146 (2013).
- 449 28. I. V. Kirstein, A. Wichels, G. Krohne, G. Gerds, Mature biofilm communities on
450 synthetic polymers in seawater - Specific or general? *Marine Environmental Research*
451 **142**, 147-154 (2018).
- 452 29. K. Keszy, S. Oberbeckmann, B. Kreikemeyer, M. Labrenz, Spatial Environmental
453 Heterogeneity Determines Young Biofilm Assemblages on Microplastics in Baltic Sea
454 Mesocosms. *Frontiers in Microbiology* **10** (2019).
- 455 30. K. L. Dudek, B. N. Cruz, B. Polidoro, S. Neuer, Microbial colonization of microplastics
456 in the Caribbean Sea. *Limnology and Oceanography Letters* **5**, 5-17 (2020).
- 457 31. E. Curren, S. C. Y. Leong, Profiles of bacterial assemblages from microplastics of
458 tropical coastal environments. *Science of The Total Environment* **655**, 313-320 (2019).
- 459 32. J. A. Bryant *et al.*, Diversity and Activity of Communities Inhabiting Plastic Debris in the
460 North Pacific Gyre. *mSystems* **1** (2016).
- 461 33. A. C. Leri, L. M. Mayer, K. R. Thornton, B. Ravel, Bromination of marine particulate
462 organic matter through oxidative mechanisms. *Geochimica et Cosmochimica Acta* **142**,
463 53-63 (2014).
- 464 34. D. Li, C.-M. Liu, R. Luo, K. Sadakane, T.-W. Lam, MEGAHIT: an ultra-fast single-node
465 solution for large and complex metagenomics assembly via succinct de Bruijn graph.
466 *Bioinformatics* **31**, 1674-1676 (2015).
- 467 35. S. Hunter *et al.*, InterPro: the integrative protein signature database. *Nucleic Acids*
468 *Research* **37**, D211-D215 (2009).
- 469 36. M. Yiğitoğlu, M. Arslan, Selective removal of Cr(VI) ions from aqueous solutions
470 including Cr(VI), Cu(II) and Cd(II) ions by 4-vinyl pyridine/2-hydroxyethylmethacrylate
471 monomer mixture grafted poly(ethylene terephthalate) fiber. *Journal of Hazardous*
472 *Materials* **166**, 435-444 (2009).

473

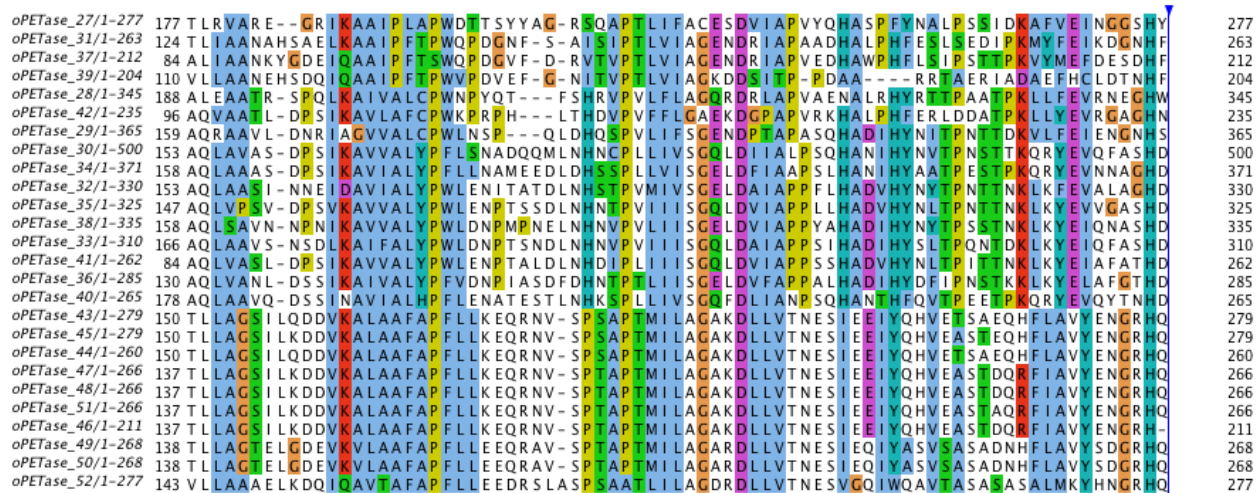
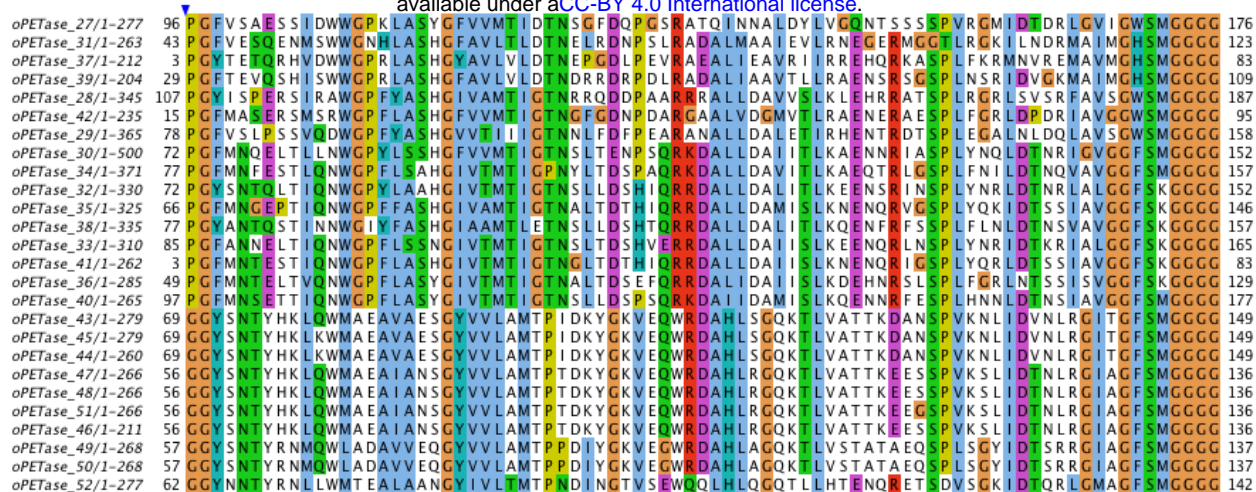
474

Figure 2 supplement 1.

A.



B.



C.



Fig 2 Supplementary 1. Alignments of ocean PETase groups M5 (A), M4(B) and M3 (C) showing conservation and variation in key PETase residues particularly catalytic tirade, aromatic clamp and oxyanion hole.

bioRxiv preprint doi: <https://doi.org/10.1101/2020.09.07.285692>; this version posted September 9, 2020. The copyright holder for this preprint (which was not certified by peer review) is the author/funder, who has granted bioRxiv a license to display the preprint in perpetuity. It is made available under a [CC-BY 4.0 International license](#).